

COGNITIVE MIMO SONAR BASED ROBUST TARGET DETECTION FOR HARBOUR AND MARITIME SURVEILLANCE APPLICATIONS

Albert Ortiz^(a), Wenhua Li, Genshe Chen, Xiaokun Li, Mo Wei^(b), Li Bai^(c),

^(a)NAVYSEA Warfare Centers

^(b)DCM Research Resources, LLC

^(c)ECE, Temple University

^(a) Albert.ortiz@navy.mil, ^(b) {wli, gchen, xli, mwei}@dcmresearchresources.com, ^(c) lbai@temple.edu

ABSTRACT

Robust detection of various hostile threats is vital to protect Navy ships and other facilities under harbour and maritime environments. Traditional single-input single-output (SISO) sonar transmits single acoustic waveform by single projector, which has a few disadvantages including low target detection probability, low resolution, vulnerability of interception by the enemy, sensitivity to jamming, etc. Multi-input multi-output (MIMO) sonar is an emerging technology to overcome all these disadvantages. In this paper, cognitive monostatic/bistatic/multistatic MIMO sonar approaches are proposed. MIMO sonar transmits different orthogonal acoustic waveforms from multiple projectors with different spatial distribution. Through space-time-waveform diversity, MIMO sonar is able to apply coherent processing techniques over the received signals, and acquires more diversity gains. The cognition concept proposed in the literature for radar and wireless communication is applied to MIMO sonar to improve its robustness and adaptability. The advantages of proposed cognitive MIMO sonar will be demonstrated by Monte Carlo computer simulations.

Keywords: cognitive MIMO sonar, space-time-waveform adaptive processing (STWAP), target detection, monostatic/bistatic/multistatic, harbour and maritime surveillance

1. INTRODUCTION

There are many threats such as submarines, mines, unmanned underwater vehicles (UUVs), unmanned surface vehicles (USV), manned surface vehicles (MSV) to Navy ships and other important facilities under harbour and maritime environments. All-weather day-night robust detection of underwater and surface threat targets is very important for military applications in the presence of severe clutter, jamming, and some kinds of sonar measurement errors. Sonar has been widely investigated in the last few decades and exploited for target detection, tracking, classification and imaging. According to the numbers of transmitters and receivers, sonar mainly has four schemes: (1) single-input single output (SISO); (2) single-input multiple-output (SIMO); (3) multi-input single-output (MISO); (4) multi-input

multi-output (MIMO) (Akyildiz 2005, Li 2008, Coon 2008, Maiwald 2008, Guerci 2003).

SISO is the most traditional sonar working approach which transmits single acoustic waveform by single projector. It has a few disadvantages including low target detection probability, low resolution, vulnerability of interception by the enemy, sensitivity to jamming, etc. SIMO sonar transmits single acoustic waveform by single projector but the received acoustic waveforms are coherently processed by the multiple receivers. Multiple-input multiple-output (MIMO) radar and sonar has recently become a hot research area for its potential advantages (Xu 2007, Li 2007, Yang 2007, Lehmann 2006). MIMO sonar uses multiple antennas to simultaneously transmit several linearly independent acoustic waveforms and deploy multiple antennas to receive the reflected signals. The echoes from different targets can be linearly independent of each other.

According to the location of transmitters and receivers, sonar can be divided into three categories: (1) monostatic sonar whose transmitters and receivers are co-located; (2) bistatic/multistatic sonar whose transmitters and receivers are distributed in different places; (3) hybrid multistatic sonar in which part of the transmitters and receivers are co-located and others are located in different places. At present the most popular sonar in use is the monostatic sonar because it is easier to operate. However, there are some disadvantages of monostatic sonar. The first is its comparatively lower survivability because it is easy to be detected by the enemy when in operation. Its resolution is limited by the size of the sonar aperture. Bistatic sonar has some advantages over monostatic sonar such as covert receiver, higher survivability, and improved ECCM. Multistatic sonar is initially defined as netted configurations of bistatic sonars (Tsakalides 1999). Recently the multistatic sonar concept is generalized to consist of different kinds of netted sonars such as conventional SIMO monostatic sonars, SIMO bistatic sonars, multiple-input-single-output (MISO) monostatic sonars, MISO bistatic sonars, and most recently proposed monostatic/bistatic/sparse-aperture MIMO sonars. Multistatic sonar has many advantages over monostatic and bistatic sonars but with more complexity and communication capacity requirements. The illuminators installed on a high valued ISR

platform and those on each monostatic sonar can provide space-time-waveform diversity with the potential of improved SNR, wider coverage, anti-jamming, and higher detection rates and lower false alarm rates, and higher resolution because of much bigger sonar aperture.

There are important and challenging problems still needed to be solved, especially for monostatic/bistatic/multistatic sonar. In this paper, we try to improve the robustness of target detection by monostatic and bistatic MIMO sonars through artificial intelligence. Cognitive radar is a very newly proposed technique (Haykin 2006). Through cognition, the sensor working status and environment sensing such as jamming can be obtained. The sonar system bias, sonar element failure, and jamming information is integrated with the space-time-waveform adaptive processing module which can greatly improve the robustness performance of MIMO sonar based target detection.

The paper is organized as follows. Section 2 presents robust STAP for cognitive monostatic SIMO sonar. Cognitive monostatic and bistatic MIMO sonars are described in Section 3 and 4, respectively. Robust target detection by cognitive MIMO sonar is developed in Section 5. Monte Carlo computer simulation is presented in Section 6. Finally, the conclusions are provided in Section 7.

2. ROBUST STAP FOR COGNITIVE MONOSTATIC SIMO

Space-time adaptive processing (STAP) is an important module of the SIMO sonar. The output of the STAP module is input into the target detection module (discussed in Section 5). The basic structure of the second-order statistics based STAP beamformer is shown in Figure 1. Without loss of generality, we consider a uniform linear array (ULA) with N -element. A coherent processing interval (CPI) consists of M pulses with a fixed repetition interval (PRI) T . Many techniques can be easily extended to nonuniform linear array, rectangle array, circular array, and other array structures. For a N -element ULA, the steering vector of the i -th waveform ($i = 1$ for SIMO sonar) is given by

$$\mathbf{s}_i = \mathbf{b}_i \otimes \mathbf{a}_i \quad (1)$$

where \otimes denotes the Kronecker product, and its N -dimensional spatial steering vector \mathbf{a}_i and M -dimensional Doppler steering vector \mathbf{b}_i are defined as

$$\mathbf{a}_i = \begin{bmatrix} 1 & e^{j2\pi d \cos \theta / \lambda_i} & \dots & e^{j2\pi(N-1)d \cos \theta / \lambda_i} \end{bmatrix}, \quad (2)$$

$$\mathbf{b}_i = \begin{bmatrix} 1 & e^{j2\pi T f_{d_i}} & e^{j2\pi T(2)f_{d_i}} & \dots & e^{j2\pi T(M-1)f_{d_i}} \end{bmatrix} \quad (3)$$

where θ is the wavefront angle, f_{d_i} is the Doppler frequency for the i -th orthogonal waveform. The original statistics based STAP algorithm is given by

$$\min_{\mathbf{w}} \mathbf{w}_i^H \mathbf{R}_{n,i} \mathbf{w}_i \quad s.t. \quad \mathbf{w}_i^H \mathbf{s}_i = 1 \quad (4)$$

where $\mathbf{R}_{n,i}$ is the positive-definite $NM \times NM$ dimensional covariance matrix for the i -th waveform which is associated with the total interference (clutter plus jamming plus receiver noise) for the given range cell under test. The optimal weight and filter output y_i for the i -th waveform are given by

$$\hat{\mathbf{w}}_i = \left(\mathbf{R}_{n,i}^{-1} \mathbf{s}_i \right) / \left(\mathbf{s}_i^H \mathbf{R}_{n,i}^{-1} \mathbf{s}_i \right), \quad (5)$$

$$y_i = \hat{\mathbf{w}}_i^H \mathbf{x}_i. \quad (6)$$

The original second-order statistics based STAP algorithm given by equation (4) is not robust to steering vector error, array element failure, jamming, and clutter. It has been shown that prior knowledge can improve the performance of STAP radar detection effectively. Cognitive STAP is proposed here to robustly detect targets for sonars. Prior knowledge and online learning of environments are both utilized to improve the detection performance. Prior knowledge is used to help selecting the secondary data. Some constraints are also formed for STAP beamformer from prior knowledge. The steering error is calibrated by the sensor registration module. Sensor health monitoring module can detect the health of each array element. The failure element is not included in the STAP beamformer. The cognitive statistics based STAP beamformer is expressed as

$$\begin{aligned} \min_{\mathbf{w}} \mathbf{w}_i^H \mathbf{R}_{n,i} \mathbf{w}_i \quad s.t. \quad & \mathbf{w}_i^H \hat{\mathbf{s}}_i = 1, \\ & \mathbf{w}_i^H \mathbf{U}_c = 0, \quad \mathbf{w}_i^H \mathbf{U}_{jam} = 0, \quad \mathbf{w}_i^H \mathbf{w}_i \leq \varepsilon \end{aligned} \quad (7)$$

where $\hat{\mathbf{s}}_i$ is the steering vector after calibration of the sensor system bias parameter $\Delta\theta$,

$$\hat{\mathbf{a}}_i = \begin{bmatrix} 1 & e^{j2\pi d \cos(\theta - \Delta\theta) / \lambda_i} & \dots & e^{j2\pi(N-1)d \cos(\theta - \Delta\theta) / \lambda_i} \end{bmatrix} \quad (8)$$

$$\hat{\mathbf{s}}_i = \mathbf{b}_i \otimes \hat{\mathbf{a}}_i. \quad (9)$$

\mathbf{U}_c is the prior knowledge of the dominant clutter subspace, \mathbf{U}_{jam} is the jamming subspace detected online by the spectrum sensing module. The failure array element detected by the sensor health monitoring has been excluded from the angle-Doppler steering

vector. The quadratic constraint expressed by equation (7) can improve the robustness of the STAP beamformer against channel mismatch and steering errors. The covariance matrix $\mathbf{R}_{n,i}$ is estimated by

$$\hat{\mathbf{R}}_{n,i} = \sum_{k=1}^K \mathbf{x}_{k,i} \mathbf{x}_{k,i}^K \cdot \quad (10)$$

Prior knowledge (GIS, clutter model database, MIMO sonar waveform library) and online learning of environments (sonar system bias, sonar health monitoring, jamming) are used to adaptively select the secondary data.

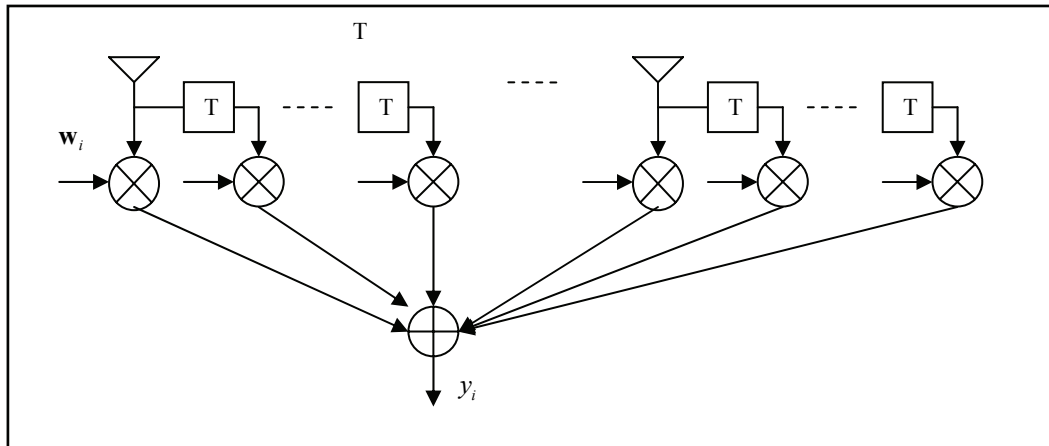


Figure 1: The Basic Structure Of The STAP Beamformer

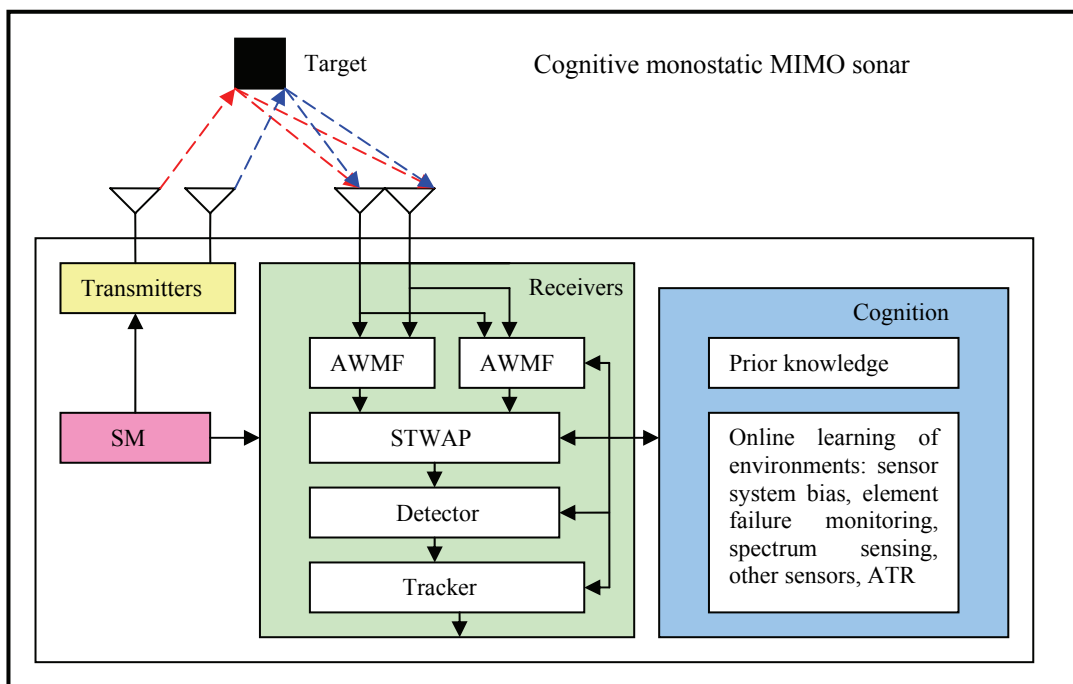


Figure 2: Block Diagram Of The Cognitive Monostatic MIMO Sonar

Many optimization algorithms proposed in the literature can be used to solve the STAP problems expressed as equations (4) and (7). Some popular methods are SMI, constrained LMS (CLMS), constrained RLS (CRLS), Generalized Sidelobe Canceller (GSC), and neural network based optimization methods. The criteria (4) and (7) optimize the output variance subject to constraints. It is not very

robust to non-Gaussian heavy-tailed clutter. A more robust STAP beamformer is based on lower order statistics such as fractional lower-order statistics (FLOS) or zero-order statistics (ZOS). The FLOS based STAP beamformer is defined as

$$\min_{\mathbf{w}} E \left\{ \left| \mathbf{w}_i^H \mathbf{x} \right|^p \right\} \quad s.t. \quad \mathbf{w}_i^H \hat{\mathbf{s}}_i = 1, \quad (11)$$

$$\mathbf{w}_i^H \mathbf{U}_c = 0, \quad \mathbf{w}_i^H \mathbf{U}_{jam} = 0, \quad \mathbf{w}_i^H \mathbf{w}_i \leq \varepsilon$$

$$\min_{\mathbf{w}} E \left\{ \log \left(\left| \mathbf{w}_i^H \mathbf{x} \right| \right) \right\} \quad s.t. \quad \mathbf{w}_i^H \hat{\mathbf{s}}_i = 1, \quad (12)$$

$$\mathbf{w}_i^H \mathbf{U}_c = 0, \quad \mathbf{w}_i^H \mathbf{U}_{jam} = 0, \quad \mathbf{w}_i^H \mathbf{w}_i \leq \varepsilon$$

where p is the fractional lower-order. When $p = 2$, FLOS based STAP becomes the second-order statistics based STAP in equation (7). The ZOS based STAP beamformer is defined by

There are no closed form solution to (11) and (12). A stochastic gradient method or Genetic Algorithms (GA) can be used with the results of (4) or (7) as its initialization.

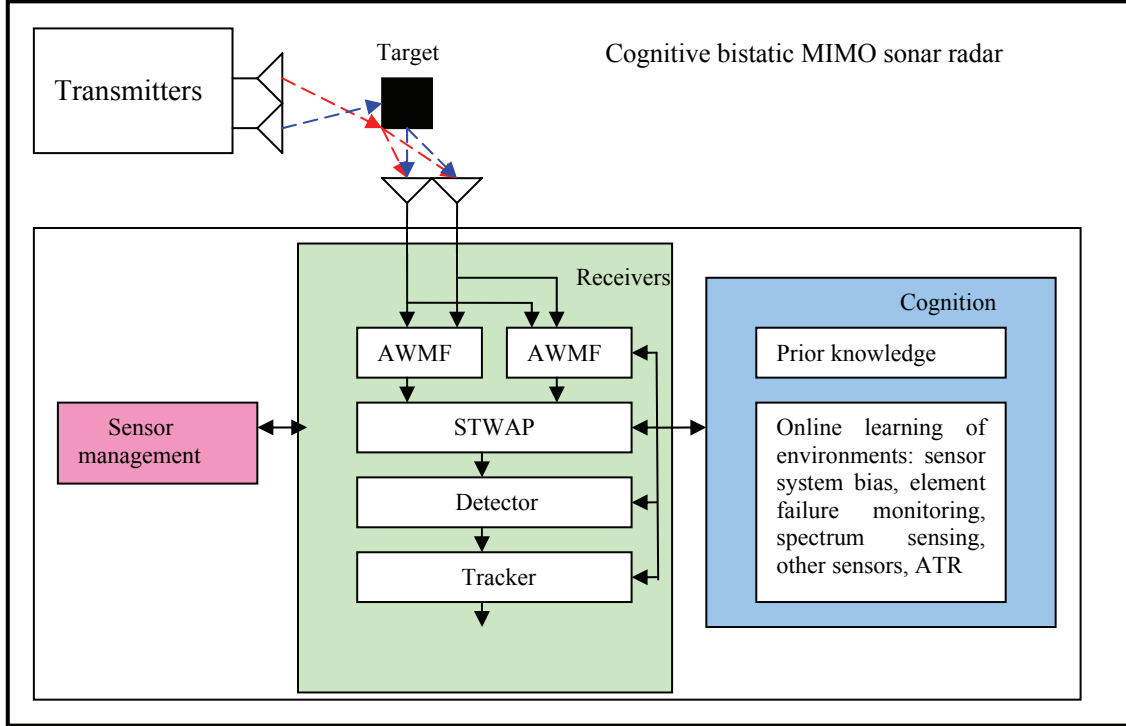


Figure 3: Block Diagram Of The Cognitive Bistatic MIMO Sonar

3. COGNITIVE MONOSTATIC MIMO SONAR

The block diagram of the cognitive monostatic MIMO sonar is shown in Figure 2. There are mainly four modules: (1) multiple transmitters; (2) co-located multiple receivers: acoustic waveform matching filter (AWMF), space-time-waveform adaptive processing (STWAP), target detector, and tracker; (3) cognition module: prior knowledge and online sensing of environments; (4) sensor management (SM). The STWAP is described in detail here.

Multiple transmitters and multiple receivers are co-located which can be two ULAs or the same ULA for both transmitting and receiving. Suppose that the element distances for the transmitter and receiver ULAs are d_T and d_R , respectively. Monostatic MIMO processes all waveforms together by a single STWAP instead of using one STAP for each waveform. Suppose there are L transmitters, N receivers, and M coherent pulses. T is the coherent pulse interval. (θ, ϕ) is the

wavefront angle of the target in 3D space to the ULA. Statistics based STWAP can be expressed as:

$$\min_{\mathbf{w}} \mathbf{w}^H \mathbf{R}_n \mathbf{w} \quad s.t. \quad \mathbf{w}^H \hat{\mathbf{s}} = 1, \quad (13)$$

$$\mathbf{w}^H \mathbf{U}_c = 0, \quad \mathbf{w}^H \mathbf{U}_{jam} = 0, \quad \mathbf{w}^H \mathbf{w} \leq \varepsilon$$

where

$$\mathbf{R}_n = E \left[\mathbf{X} \mathbf{X}^H \right], \quad (14)$$

(\mathbf{X} is the NML -dimensional baseband measurements.)

$$\mathbf{w} = [\mathbf{w}_1^T, \mathbf{w}_2^T, \dots, \mathbf{w}_L^T]^T \text{ (weight)}, \quad (15)$$

$$\hat{\mathbf{s}} = [\hat{\mathbf{s}}_1^T, \hat{\mathbf{s}}_2^T, \dots, \hat{\mathbf{s}}_L^T]^T, \quad (16)$$

(steering vector after sensor calibration),

$$\hat{\mathbf{s}}_l = \mathbf{b}_l \otimes \hat{\mathbf{a}}_l \text{ (steering vector of } l\text{-th waveform),} \quad (17)$$

$$\mathbf{b}_l = \begin{bmatrix} 1 & e^{j2\pi T f_{d_l}} & e^{j2\pi T(2) f_{d_l}} & \dots & e^{j2\pi T(M-1) f_{d_l}} \end{bmatrix} \quad (18)$$

(Doppler steering vector of l -th waveform),

$$\mathbf{a}_l = \begin{bmatrix} 1 & \dots & e^{j2\pi(N-1)d_R \cos(\theta-\Delta\theta) \sin(\phi-\Delta\phi)/\lambda_l} \\ e^{j2\pi d_T(l-1) \cos(\theta-\Delta\theta) \sin(\phi-\Delta\phi)/\lambda_l} \end{bmatrix} \quad (19)$$

(spatial steering vector of l -th waveform),

$$f_{d_l} = \frac{2}{\lambda_l} \left[(\mathbf{v}_t - \mathbf{v}_e)(\mathbf{P}_t - \mathbf{P}_e) / |\mathbf{P}_t - \mathbf{P}_e| \right] \quad (20)$$

(Doppler frequency of l -th waveform).

If $L = 1$, monostatic MIMO in equation (13) changes to SIMO in equation (4).

4. COGNITIVE BISTATIC MIMO SONAR

The block diagram of the cognitive bistatic MIMO sonar is shown in Figure 3. Transmitters ULA and receivers ULA are located on two different platforms. There are mainly four modules: (1) multiple transmitters on one platform; (2) co-located multiple receivers on another platform: acoustic waveform matching filter (AWMF), space-time-waveform adaptive processing (STWAP), target detector, and tracker; (3) cognition module: prior knowledge and online sensing of environments; (4) sensor management (SM). The STWAP is described in detail in this section.

Suppose that the element distances for the transmitter and receiver ULAs are d_T and d_R , respectively. T is the coherent pulse interval. Suppose there are L transmitters, N receivers, and M coherent pulses. (θ_t, ϕ_t) and (θ_r, ϕ_r) are the wavefront angles of the target to the transmitter and receiver ULAs in 3D space. Statistics based bistatic MIMO STWAP can be expressed as the following optimization problem:

$$\begin{aligned} \min_{\mathbf{w}} \quad & \mathbf{w}^H \mathbf{R}_{2D,n} \mathbf{w} \quad s.t. \quad \mathbf{w}^H \hat{\mathbf{s}} = 1, \\ & \mathbf{w}^H \mathbf{U}_c = 0, \quad \mathbf{w}^H \mathbf{U}_{jam} = 0, \quad \mathbf{w}^H \mathbf{w} \leq \varepsilon \end{aligned} \quad (21)$$

where

$$\mathbf{R}_{2D,n} = E[\mathbf{X}_{2D} \mathbf{X}_{2D}^H], \quad (22)$$

\mathbf{X} is the NML -dimensional baseband measurements after 2D Doppler compensation,

$$\mathbf{w} = [\mathbf{w}_1^T, \mathbf{w}_2^T, \dots, \mathbf{w}_L^T]^T \text{ (weight),} \quad (23)$$

$$\hat{\mathbf{s}} = [\hat{\mathbf{s}}_1^T, \hat{\mathbf{s}}_2^T, \dots, \hat{\mathbf{s}}_L^T]^T \text{ (steering vector),} \quad (24)$$

$$\hat{\mathbf{s}}_l = \mathbf{b}_l \otimes \hat{\mathbf{a}}_l \text{ (steering vector of } l\text{-th waveform),} \quad (25)$$

$$\mathbf{b}_l = \begin{bmatrix} 1 & e^{j2\pi T f_{d_l}} & e^{j2\pi T(2) f_{d_l}} & \dots & e^{j2\pi T(M-1) f_{d_l}} \end{bmatrix}, \quad (26)$$

(Doppler steering vector of l -th waveform),

$$\hat{\mathbf{a}}_l = \begin{bmatrix} 1 & \dots & e^{j2\pi(N-1)d_R \cos \bar{\theta}_R \sin \bar{\phi}_R / \lambda_l} \\ e^{j2\pi d_T(l-1) \cos \bar{\theta}_T \sin \bar{\phi}_T / \lambda_l} \end{bmatrix}, \quad (27)$$

(l -th spatial steering vector),

$$f_{d_l} = \frac{1}{\lambda_l} \left[\frac{(\mathbf{v}_t - \mathbf{v}_e)(\mathbf{P}_t - \mathbf{P}_e) / |\mathbf{P}_t - \mathbf{P}_e| + (\mathbf{v}_r - \mathbf{v}_t)(\mathbf{P}_r - \mathbf{P}_t) / |\mathbf{P}_r - \mathbf{P}_t|}{2} \right] \quad (28)$$

(Doppler frequency of l -th waveform).

Multistatic MIMO sonar can be set up with networked multiple monostatic and bistatic MIMO sonars. We will present our multistatic MIMO sonar in our future paper.

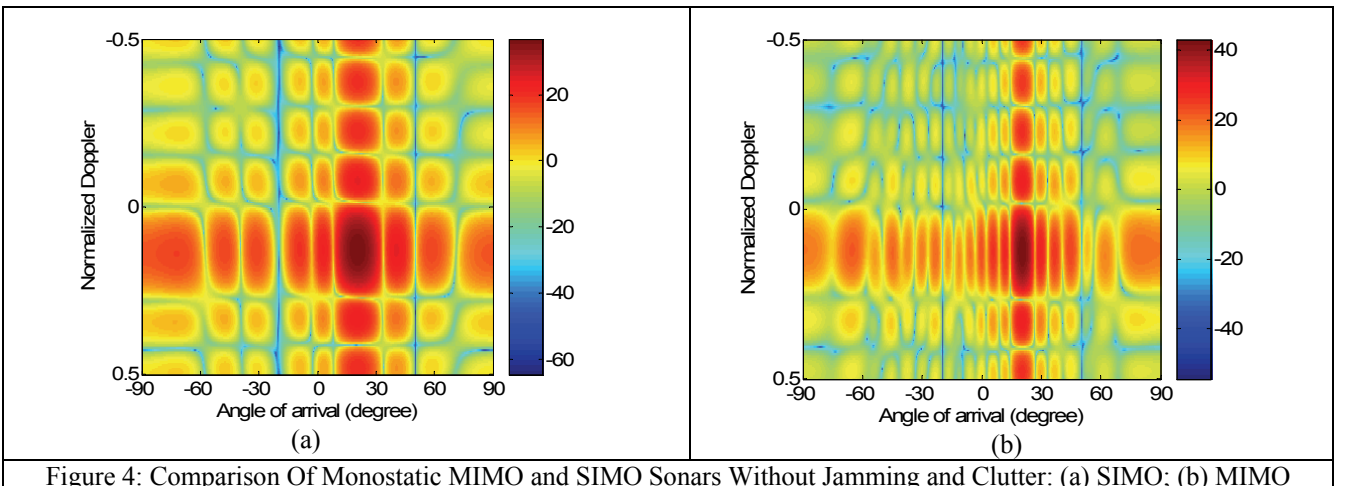


Figure 4: Comparison Of Monostatic MIMO and SIMO Sonars Without Jamming and Clutter: (a) SIMO; (b) MIMO

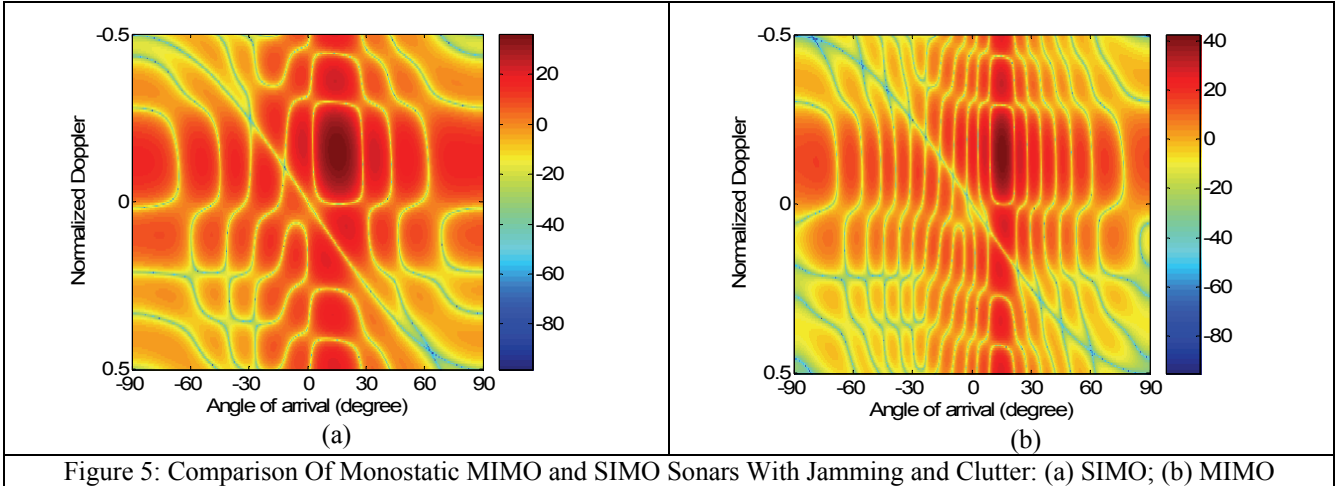


Figure 5: Comparison Of Monostatic MIMO and SIMO Sonars With Jamming and Clutter: (a) SIMO; (b) MIMO

5. ROBUST TARGET DETECTION BY COGNITIVE MIMO SONAR

Distributed detection is presented here for the multistatic sonar with a configuration of many monostatic and bistatic sonars. There are three steps: (1) Optimal weight estimation by STAP/STWAP for each tested range cell. (2) Local adaptive matched filter (AMF) constant false alarm rate (CFAR) detection using the estimated weight (Goldstein 1999). (3) Detection fusion in the Fusion Center by DS reasoning. The sonar detection for the k -th tested range cell and i -th STAP/STWAP can be expressed for each of the following two hypotheses,

$$\begin{aligned} H_0 : \mathbf{x}_i^k &= n_i^k, \\ H_1 : \mathbf{x}_i^k &= \mathbf{x}_i^k + n_i^k. \end{aligned} \quad (29)$$

The adaptive matched filter (AMF) CFAR test statistic Λ_i^k is then calculated by

$$\Lambda_i^k = \left\| (\hat{\mathbf{w}}_i^k)^H \mathbf{x}_i^k \right\|^2 \left[(\hat{\mathbf{s}}_i^k)^H (\hat{\mathbf{R}}_i^k)^{-1} \hat{\mathbf{s}}_i^k \right]. \quad (30)$$

The local detection result is

$$D_i^k = \begin{cases} H_1 : \text{if } \Lambda_i^k \geq \eta_i^k, \\ H_0 : \text{if } \Lambda_i^k < \eta_i^k. \end{cases} \quad (31)$$

The local AMF CFAR detection results are finally fused by our DS fusion toolbox.

6. MONTE CARLO COMPUTER SIMULATIONS

The performance of cognitive MIMO sonar is evaluated and compared with conventional SIMO sonar under various environments. Linear sonar arrays are used for MIMO transmitter and receiver. The proposed method

can also be applied to other sonar arrays such as rectangular and three-dimensional sonar arrays.

Figure 4 compares the performance of SIMO and monostatic MIMO sonars without jamming and clutter (only random noise exists in the measurements). In Figure 4(a), there are 10-element for MO. In Figure 4(b), there are 2-element for MI and 10-element for MO. Figure 4 shows that through waveform diversity, the resolution of MIMO sonars is improved effectively. The resolution of 2-input 10-output sonar is 2 times higher than that of 1-input 10-output SIMO sonars.

Figure 5 compares the performance of cognitive SIMO and monostatic MIMO sonars with jamming and clutter. In Figure 5(a), there are 10-element for MO. In Figure 5(b), there are 2-element for MI and 10-element for MO. Through cognitive sensing of the environments, the covariance of the jammings and clutters are available and applied in the space-time-waveform adaptive processing algorithm. Figure 5 shows that through waveform diversity, the resolution of MIMO sonars is also improved effectively under jamming and clutter. Deep notches are formed to filter the jamming and clutter. As shown in Figure 4 and Figure 5, the output of the SIMO and MIMO sonars at the target 's position and Doppler has a peak. After STWAP, the target can be detected by CFAR.

7. CONCLUSIONS

Inspired by recent advances in MIMO radar and cognitive radar, we have developed a robust target detection based on cognitive monostatic and bistatic MIMO sonar for harbour and maritime surveillance applications. STWAP, target detector and cognition are three important modules in a MIMO sonar. It has been shown that through space-time-waveform diversity and cognition processing, MIMO sonar has many superior advantages over conventional SISO sonar such as higher target detection probability, higher resolution, much less vulnerability of interception by the enemy, more robustness to jamming and sonar system bias and sonar element failure. More complex networked

multistatic MIMO sonar is in investigation and the new results will be reported in another paper.

REFERENCES

- Akyildiz, I. F., Pompili, D., and Melodia, T., 2005. Underwater acoustic sensor networks: research challenges. *Ad Hoc Networks*, 3, 257-279.
- Li, Y., Huang, H., Li, S., and Zhang, C., 2008. LPI Performance analysis of MIMO sonar detection. *UDT Europe 2008*.
- Coon, A. Hall, B., Kanyuck, B., and Skarda, G., 2008. Novel approaches to multistatic sonar processing and source deployment. *UDT Europe 2008*.
- Maiwald, D., Benen, S., Corsten, A., Rose, B., and Schmidt-Schierhorn, H., 2008. Modular multistatic sonar systems. *UDT Europe 2008*.
- Nicholas J. Willis, 2005. *Bistatic Radar*. Scitech Publishing, Inc.
- Guerci, J., 2003. *Space-Time Adaptive Processing for Radar*. Artech House.
- Goldstein, J. S., Reed, I., and Zulch, P., 1999. Multistage partially adaptive CFAR detection algorithm. *IEEE Trans. AES*, 35(2), 645-661.
- Tsakalides, P., and Nikias, L., 1999. Robust space-time adaptive processing (STAP) in non-Gaussian clutter environments. *IEE Proc. – Radar, Sonar Navig.*, 146(2), 84-93.
- Haykin, S., 2006. Cognitive radar: a way of the future, *IEEE Signal Processing Magazine*, 23(1), 30-40.
- Xu, L., and Li, L., 2007. Iterative generalized likelihood ratio test for MIMO radar. *IEEE Transactions on Signal Processing*, 55(6), 2375-2385.
- Li, J., and Stoica, P., 2007. MIMO radar with colocated antennas: review of some recent work. *IEEE Signal Processing Magazine*, 24(5), 106-114.
- Yang, Y., and Blum, R. S., 2007. Minimax robust MIMO radar waveform design. *IEEE Journal of Selected Topics in Signal Processing*, special issue on: *Adaptive Waveform Design for Agile Sensing and Communication*, 147-155.
- Lehmann, N., Haimovich, A., Blum, R., Chizhik, D., Cimini, L., and Valenzuela, R., 2006. High resolution MIMO-radar. *Proceedings of Asilomar Conference on Signals, Systems and Computers*, Pacific Grove, CA, November 2006.
- Haykin, S.. Cognitive radar network, ieeexplore.ieee.org/iel5/11178/36018/01706227.pdf